High-Resolution Spectroscopy of T Tauri Stars

Taguchi, Yuske
Itoh, Yoichi
Mukai, Tadashi

(Citation)
Publications of the Astronomical Society of Japan,61(2):251-258

(Issue Date)
2009-04-25

(Resource Type)
journal article

(Version)
Version of Record

(URL)
https://hdl.handle.net/20.500.14094/90001421

PASJ: Publ. Astron. Soc. Japan **61**, 251–258, 2009 April 25

High-Resolution Spectroscopy of T Tauri Stars

Yuske TAGUCHI,* Yoichi ITOH, and Tadashi MUKAI
Graduate School of Science and Technology, Kobe University, 1-1 Rokkodai-cho, Nada-ku, Kobe 657-8501
yuske@harbor.scitec.kobe-u.ac.jp

(Received 2005 March 23; accepted 2008 November 12)

Abstract

We have conducted high-resolution spectroscopic observations of a sample of both classical and weak-line T Tauri stars embedded in the Taurus-Auriga molecular cloud using the Okayama Astrophysical Observatory's 188 cm telescope equipped with HIDES (HIgh Dispersion Echelle Spectrograph). Utilizing the ratios of equivalent widths of specific lines, we efficiently eliminated the effects of "veiling" and determined the atmospheric parameters individually for each object. Eight pairs of temperature-sensitive line-ratios were selected to derive the effective temperature with high precision and reliability. As for the surface gravity, we have developed a new method to determine the value. The method was first tested on observed spectral standards, and the derived surface gravities had a less than 5% deviation from the values in the literature. The derived surface gravities are well within the range of the assumed values for T Tauri stars.

Key words: stars:pre-main-sequence — fundamental parameters — spectroscopy

1. Introduction

To understand the properties of T Tauri stars (TTSs) is an utmost priority to comprehend the evolution of stellar objects, and also the formation and evolution of extrasolar planets. The fundamental atmospheric parameters, effective temperature ($T_{\rm eff}$), surface gravity ($\log g$), and metallicity ([Fe/H]), are useful indicators that can give us valid information on the TTS at hand. The effective temperature and the surface gravity may be considered to be more important, since the two parameters will determine the position of the object on the HR diagram, and also lead to determine the age and mass.

There have been much research in the past attempting to determine the two parameters for TTSs, starting with photometric methods. Cohen and Kuhi (1979) were the first to catalogue a vast sample of TTSs from several star-forming regions. Their work has been followed by many other researchers, such as Strom et al. (1989), Kenyon and Hartmann (1995), Calvet et al. (2004). There is still much room for improvements to be made concerning the photometric method to derive the fundamental parameters of TTSs. One of the biggest challenges is to remove any effects brought about by the circumstellar matter surrounding the central object, known as "veiling".

The veiling continuum is known to stretch out shortward to the UV region and longward to the IR, where the radiation is considered to originate from the accretion shock region and the circumstellar disk, respectively (Kenyon & Hartmann 1987; Bertout et al. 1988). In the optical range, the main source of veiling is considered to be an almost featureless nonstellar continuum, which reduces the depth of the photospheric absorption lines (Basri & Batalha 1990; Hartigan et al. 1991). The level of veiling seems to correlate with the activeness of the accretion disk (Bertout 1989), which explains the absence of veiling in weak-line TTSs. Finkenzeller and Basri (1987) have pointed out that a chromospheric "filling-in" of selective absorption lines is also one such effect of veiling. Because of the presence of veiling, photometric methods to determine the stellar parameters of TTSs would be inaccurate. As mentioned in Padgett (1996), the effective temperature and surface gravity determinations based on colors and flux would lead to false results, especially for the young objects with active accretion.

Because the effects of veiling can not be ignored, spectroscopic methods are preferred for deriving the fundamental parameters of TTSs. The level of veiling can be estimated to be an equal amount within a narrow wavelength range (~ 10 Å). Since the equivalent width (EW) is defined as the flux of the line divided by the continuum level, taking the ratio of the EW of close by features will cancel out the level of the continuum, resulting in the elimination of veiling. Basri and Batalha (1990) were the first to utilize high-resolution spectroscopic observations to determine the spectral types of TTSs. They used two pairs of line-ratios, Fe I λ5706/V I λ5707 and Fe I λ6200/Sc I λ6210, to assign spectral types for a number of TTSs from the Taurus-Auriga region. Schiavon, Batalha, and Barbuy (1995) also used the pair λ5707/λ5706 along with two new pairs, CaH λ6796/Fe I λ5706 and CaH λ6796/V I λ5707, to directly derive the effective temperature and surface gravity of TTSs. Padgett (1996) utilized a total of 5 pairs of line-ratios, V I λ6199/Fe I λ6200, Fe I λ6200/V I λ6216, V I λ6119/Fe I λ6200, V I λ6119/Fe I λ6219, and Fe I λ6705/Fe I λ6703, to precisely determine the effective temperature of 30 Weak-Line TTSs embedded in seven star-forming regions.

As for determining the surface gravity of TTSs, only Schiavon et al. (1995) have derived individual values for TTSs by making use of high-resolution spectroscopy. Due to the effects of veiling, values derived through photometric methods would yield an improper value.

This paper presents determinations of the effective temperature and surface gravity of TTSs embedded in the

* Present address: Hitachi Software Engineering Co. Ltd., 4-12-7 Higashi-Shinagawa, Shinagawa-ku, Tokyo 140-0002

Table 1. List of observed T Tauri stars and their derived properties.

Star	Spectral type	R (mag)	Hα EW (Å)	Integration time	S/N	$v \sin i$ (cm s^{-2})	$T_{\rm eff}$ (K)	$\log g$ (cm s^{-2})
HBC 388	K1	9.9	0.5	1800 s × 5	∼150	∼20	5440 ± 70	4.33 ± 0.23
V773 Tau	K2	9.8	1.5	1800 s × 2	∼170	∼50	5650 ± 150	4.27 ± 0.33
UX Tau	K2	10.7	3.9	1800 s × 7	∼120	∼25	5230 ± 100	4.14 ± 0.44
GI Tau	K7	12.1	19	1800 s × 4	∼50	∼15	4460 ± 280	2.53 ± 0.97
T Tau	K1	9.1	38	600 s × 6	∼130	∼25	5070 ± 110	4.14 ± 0.38
DR Tau	K4	10.9	87	1800 s × 6	∼80	∼15	4710 ± 220	2.75 ± 0.67

Table 2. List of observed spectral standards and their properties.

HR#	Spectral type	Integration time (s)	S/N	$T_{\rm eff}$ (K)	$\log g$ (cm s^{-2})	[Fe/H]
224	K5 III	180	∼60	3918	—	−0.07
8086	K7 V	240	∼90	4252	4.60	−0.05
464	K3 III	600	∼50	4425	2.10	0.12
8085	K5 V	840	∼70	4463	4.50	−0.05
753	K3 V	1080	∼130	4775	4.60	—
7615	K0 III	180	∼100	4887	2.50	0.11
8974	K1 III–IV	180	∼100	4904	3.10	0.04
6869	K0 III–IV	420	∼160	4949	2.90	−0.08
8499	G8 III–IV	360	∼90	4956	2.80	−0.07
7957	K0 IV	90	∼190	4996	3.34	−0.17
8684	G8 III	300	∼140	5044	—	−0.14
7602	G8 IV	180	∼250	5098	3.56	−0.08
7462	K0 V	360	∼220	5253	4.50	−0.25
6623	G5 IV–V	180	∼150	5527	4.10	0.30
7504	G2.5 V	840	∼210	5664	4.40	0.00
7503	G1.5 V	600	∼220	5826	4.30	0.00
2047	G0 V	270	∼330	5842	4.41	−0.09

Taurus-Auriga molecular cloud. Making use of high-resolution spectroscopy and numerous line-ratio pairs, we efficiently eliminated the effects of veiling, and determined the two parameters for each TTS with high precision and reliability.

2. Observations

2.1. Sample Selection

A number of scientific criteria and instrumental limitations were involved in selecting TTSs suitable for analysis. First, the ability to measure relatively weak metal lines required S/N $\geq$ 50 in the continuum around 6000 Å. We were limited to observing stars with $R \lesssim 12$ mag. One of the main objects of this work was to derive the atmospheric parameters of a TTS, no matter how much the degree of photospheric veiling, and therefore the amount of veiling was not a selection factor. The selection of TTSs was based on the data supplied by a catalogue of weak-line and classical TTSs (Strom et al. 1989). A list of the observed TTSs is presented in table 1.

The current study utilized metallic absorption line ratios to determine the effective temperature of TTSs. In order to calibrate the ratios against effective temperature, a set of 18 spectral standards ranging in spectral type from G0 to K7 were selected from a list of Bell and Gustafsson (1989). Of the 18 chosen spectral calibration stars, 8 were luminosity class V, and 9 are either III or IV. After data reductions, we found that one of them (HR 7478) turned out to be a spectroscopic binary. The details of the spectral standards, excluding HR 7478, are listed in table 2.

2.2. Observation Method

We have conducted high-resolution spectroscopic observations at the Okayama Astrophysical Observatory's 188 cm telescope equipped with HIDES (HIgh Dispersion Echelle Spectrograph). This instrument is a cross-dispersed echelle spectrograph using a 2048 × 4096 pixel CCD as a detector. Equipped with an echelle grating of 31.6 gr/mm and cross-disperser of 250 gr/mm (red), we achieved a spectral resolution of ∼72000 with a slit width of 0.″76. For the current work, we used a portion of the spectral coverage from 5800 to 6800 Å.

The observations were carried out on 5 nights from 2002 November 8–12. Wavelength calibrations were performed at the beginning and end of each night, using a Thorium-Argon arc source. Comparisons between the Thorium-Argon

Table 3. Equivalent widths of lines used in effective temperature determination (mÅ).

Star	V I 6039.7	Fe I 6042.2	Fe I 6056.0	V I 6058.1	V I 6119.5	V I 6199.2
HBC 388	41 ± 3	79 ± 3	100 ± 3	11 ± 3	50 ± 6	70 ± 6
V773 Tauri	129 ± 9	94 ± 8	—	—	155 ± 18	52 ± 1
UX Tauri	—	—	110 ± 8	—	94 ± 14	93 ± 8
GI Tauri	75 ± 5	44 ± 1	63 ± 5	—	96 ± 11	144 ± 12
T Tauri	99 ± 6	108 ± 6	113 ± 6	48 ± 6	77 ± 7	107 ± 6
DR Tauri	46 ± 4	26 ± 3	27 ± 6	23 ± 3	35 ± 3	27 ± 4
Star	Fe I 6200.3	Sc I 6210.7	V I 6216.4	Fe I 6219.3	Fe I 6703.6	Fe I 6705.1
HBC 380	138 ± 3	23 ± 3	87 ± 5	143 ± 3	55 ± 5	75 ± 8
V773 Tauri	274 ± 16	44 ± 5	—	—	83 ± 15	53 ± 5
UX Tauri	146 ± 4	43 ± 45	97 ± 4	155 ± 5	71 ± 6	73 ± 7
GI Tauri	144 ± 13	133 ± 13	234 ± 16	161 ± 10	38 ± 5	61 ± 12
T Tauri	150 ± 5	57 ± 4	108 ± 6	157 ± 3	77 ± 9	69 ± 9
DR Tauri	32 ± 3	12 ± 1	39 ± 2	11 ± 2	—	—

arcs show that the wavelength calibration remained stable throughout the whole run. Among the 5 nights, there were only 3 spectroscopic nights, therefore all of the spectral standards were observed, but the number of observed TTSs was limited to 6.

3. Data Analysis and Results

3.1. Data Reduction

All of the spectroscopic data were reduced using IRAF. First, the overscan data was subtracted individually from each raw data, and then the averaged bias frame was subtracted from each image. Flat field images were obtained each night by taking exposures of a white lamp built within the HIDES instrument. The median of the flat field images was created and applied to each image taken on the same night for flat field correction. After this, the data were eliminated of any unnecessary brightness, such as scattered light and cosmic-rays. Next, each echelle order was wavelength calibrated using a Th-Ar lamp, and the spectral resolution was derived from these comparison images. The data of TTSs were combined to improve the S/N ratio. Finally, the data were normalized so that the continuum level was set to unity. The EWs of specific absorption line features were measured using a Gaussian fit to the observed absorption features.

3.2. Effective Temperature Determination

The high spectral resolution of the observations allowed the utilization of pairs of individual neutral metal lines to determine the effective temperatures of TTSs. For two absorption line features within a narrow wavelength range, the level of veiling could be estimated to be an equal amount. Therefore, if we measure the EW of closely spaced features and calculate their ratio, the continuum level will be canceled out, while eliminating the effects of veiling. Previous uses of individual line-ratios observed with high resolution spectroscopy for temperature determination included that of Basri and Batalha (1990), Schiavon et al. (1995), and Padgett (1996). In the current study, we utilized 8 pairs of temperature-sensitive line-ratios (V I λ6040/Fe I λ6042, V I λ6058/Fe I λ6056, V I λ6119/Fe I λ6200, V I λ6119/Fe I λ6219, V I λ6199/Fe I λ6200, Fe I λ6200/V I λ6216, Sc I λ6210/Fe I λ6200, and Fe I λ6705/Fe I λ6703) to determine the effective temperatures of TTSs. The 8 pairs were selected under the criteria that the lines consisting a pair have close wavelengths, and that the two lines are not blended by other near-by features. The measured EWs of the lines used in the effective temperature determination are listed in table 3.

After all of the EWs of the necessary lines were measured, a linear regression fit to the line-ratio versus $T_{\rm eff}$ relation for each line pair was determined from the spectral standard data. Next, the EW ratios measured from the TTS sample was applied to the relation to determine the "line-ratio" temperature. Linear-regression fits to the line-ratio versus effective temperature data from the spectral standards are displayed in figure 1. The error-weighted mean of all the line-ratio temperatures for each star was adopted as the effective temperature, and the root-summed square of the standard deviation between the line-ratio temperatures and the error for each line-ratio temperature is given as the uncertainty for $T_{\rm eff}$. The line-ratios of the TTS sample are displayed in figures 2. The effective temperatures derived for the TTSs embedded in the Taurus molecular cloud are listed in table 1.

3.3. Surface Gravity Determination

The surface gravity is probably one of the most difficult fundamental atmospheric parameters to determine. There have been many approaches to derive the surface gravity of TTSs conducted by much past research. In the current work, we sought to find a new method to determine the surface gravity using similar methods utilized to derive the effective temperature. That is, to use the line ratio of neutral iron to a gravity-sensitive line, ionized iron. This method is expected to give us a more certain value to the true surface gravity,

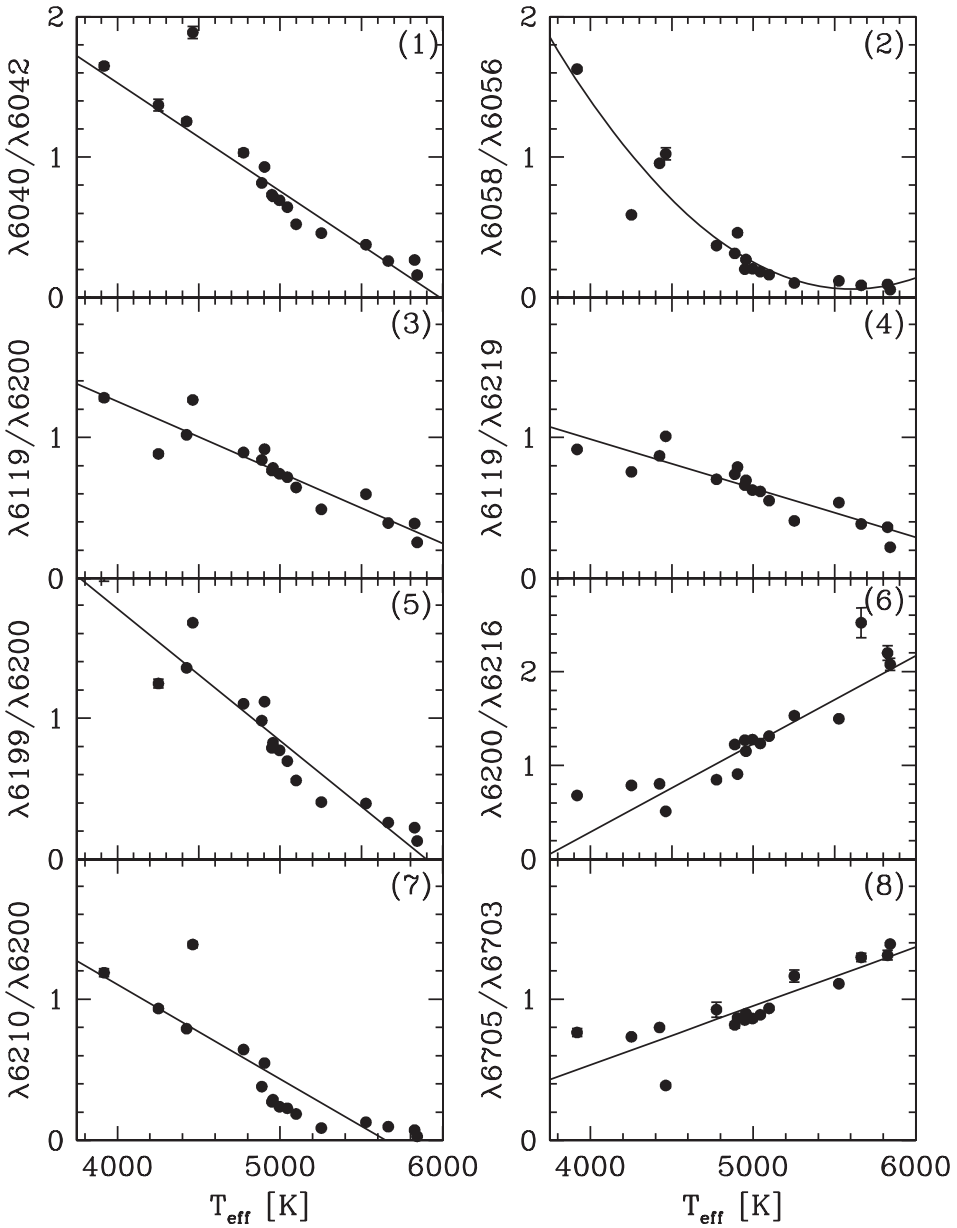

Fig. 1. Line-ratio versus effective temperature linear regression fits. The circles with error bars denote the results of the current work, and the lines the regression fits to the data.

compared to such traditional methods, like finding a model fit to the spectra of the object in debate, while ignoring the effects of veiling.

We have carefully chosen 7 pairs of neutral iron (Fe I) to ionized the iron (Fe II) ratios. In selecting these pairs, we used a modified version of the WIDTH9 program (by Yoichi Takeda: Takeda et al. 2002) that calculates the stellar spectra based on the ATLAS9 models of Kurucz (1993).

The line pairs to be used in the determination of the surface gravity $\log g$ were carefully selected as follows: (1) search for Fe II absorption features that can be clearly distinguished (unblended) in the TTSs spectra, and have well determined gf values; (2) find Fe I absorption features approximately 10 Å within the Fe II feature. Within these criteria, we were able to find 7 pairs (Fe II λ6084/Fe I λ6082, Fe II λ6084/Fe I λ6096, Fe II λ6149/Fe I λ6151, Fe II λ6238/Fe I λ6230, Fe II λ6238/Fe I λ6232, Fe II λ6247/Fe I λ6252, Fe II λ6432/Fe I λ6430) of gravity-sensitive line-ratios (figure 3).

To confirm the reliability of the newly devoloped method, we tested the procedure on the observed spectral standards. First, we produced a grid of model spectra with the known effective temperature of the observed standard, microturbulence of $1.00\,\mathrm{km\,s^{-1}}$, metallicity of ± 0.00 dex, and surface gravities ranging from 2.00–5.00 in steps of 0.5 dex. Changes in microturbulence and metallicity did not need to be considered due to the minimal effects they have on the absorption features compared to changes in the effective temperature and the surface gravity. With the line-ratios determined from the

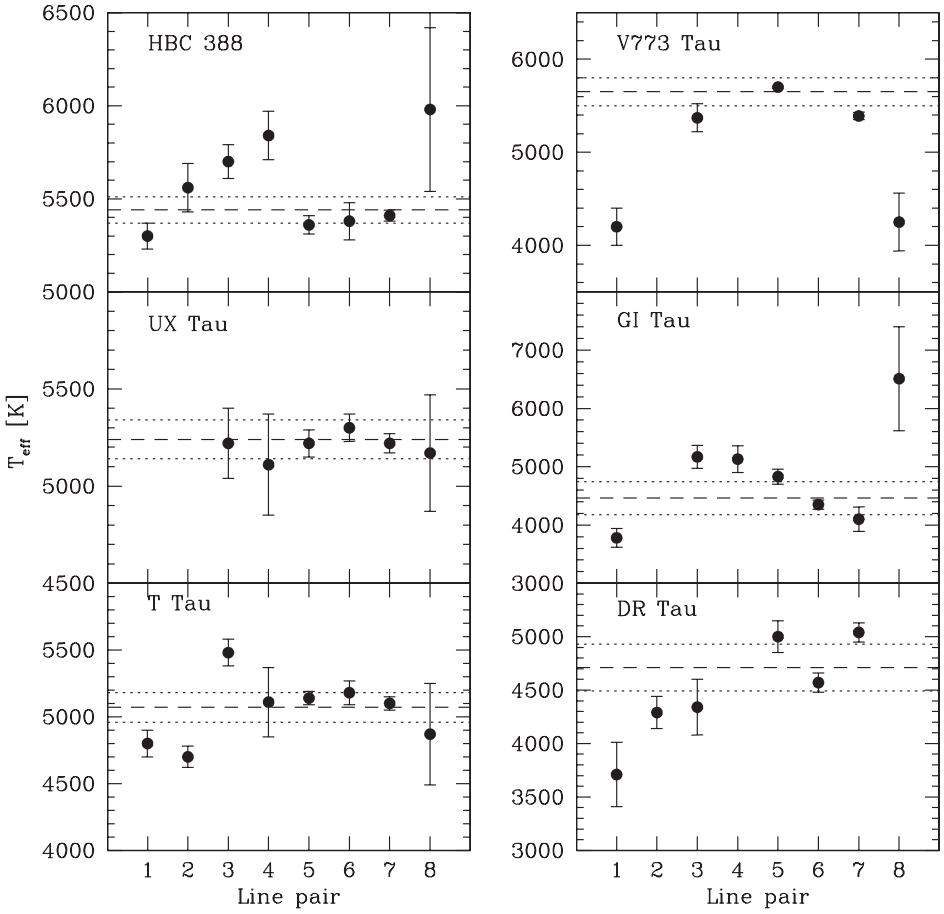

Fig. 2. Derived line-ratio effective temperatures. The error-weighted average for each object is shown as a dashed line with the uncertainty as the dotted lines. The "Line pair" numbers correspond to the numbers in parenthesis of each linear regression fit of figure 1.

measurements of the EWs for the grid of model spectra, we could derive a linear regression fit to the line-ratio versus log g relation. Plotting the line-ratio derived for the spectral standard on the line-ratio-to-log g relation yieldd a surface gravity value for that standard star. All of the derived values from the 7 ratio-to-log g relationships were then averaged using the error as weights; the root-summed square of the standard deviation between the line-ratio gravities and the error for each line-ratio gravity is given as the uncertainty of the results. We derived the surface gravity of each of the spectral standards. With the largest difference being less than 7%, the derived surface gravities were precisely averaged to within 5% compared to the values in the literature.

Now that we are confident of the reliability of the new method, we will go on to derive the surface gravity of TTSs. Using the procedure described above, but with the model spectra having the derived effective temperature of the TTS, microturbulence and metallicity fixed at 2.00 km s^{-1} and $\pm$ 0.00 dex respectively, we can now derive a line-ratio versus log g relation for that TTS. The EWs of the measured lines used for the surface gravity determination are listed in tables 4 and 5, and the line-ratio gravities are shown in figure 4. The final results are summarized in table 1.

4. Discussion

We compared the values estimated in the current work to past results. For T Tau and V773 Tau, utilizing the luminosities and effective temperatures derived in the literature, we derived the surface gravity using stellar evolutionary tracks provided by Siess et al. (1997), in which the effective temperature, surface gravity, and luminosity of an object are presented. Figure 5 displays the derived effective temperature and surface gravities for T Tau (squares) and V773 Tau (triangles) along with results from the literature.

For V773 Tau, both the effective temperature and the surface gravity are considerably different compared to past results. The cause of this difference can be explained by the high projected rotational velocity of V773 Tau. Compared to the other TTSs, where the absorption features can be clearly resolved ($v \sin i$ = 15 $\sim$ 25 km s^{-1}), V773 Tau has $v \sin i \sim$ 50 km s^{-1} which is subject to high amounts of blending. Of the absorption features that are necessary for the line-ratio measurements, many were unable to be resolved for the EW to be measured. As a consequence, 5 out of 8 line-ratio effective temperatures, and only 3 out of 7 line-ratio surface gravities were derived to calculate the final results. Therefore, the reliability of the results of V773 Tau is not firm.

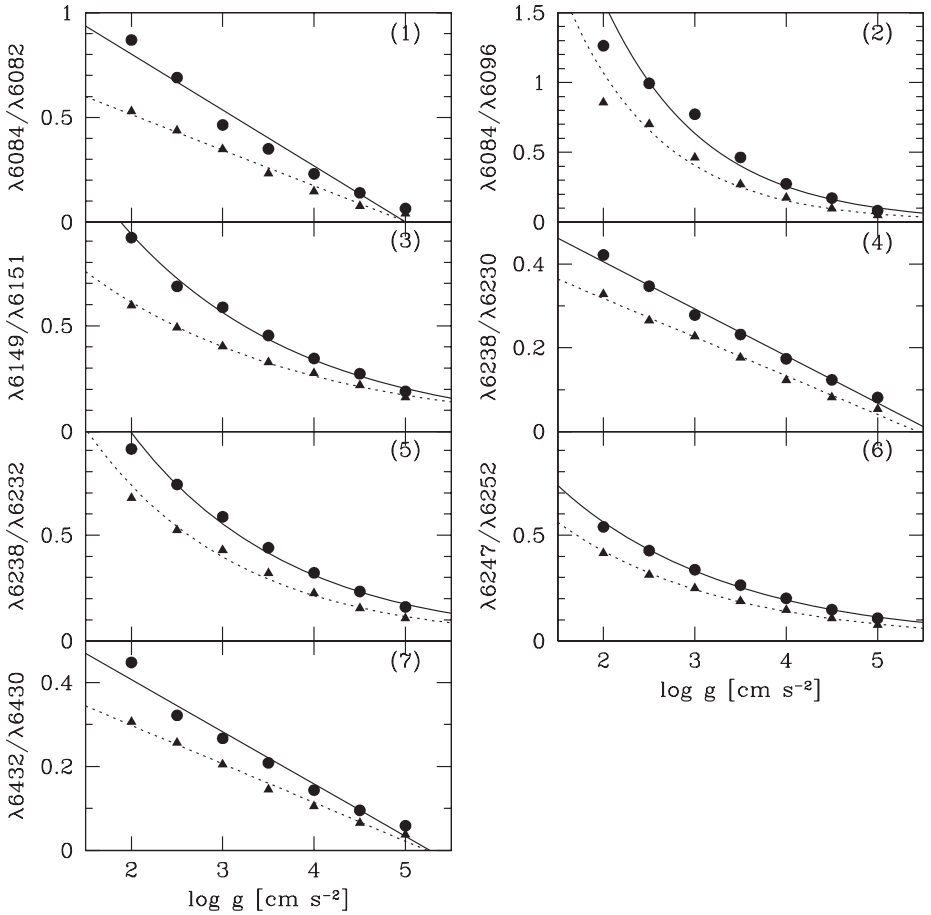

Fig. 3. Line-ratio versus surface gravity. The circles and solid lines are EWs and their fit for $T_{\rm eff} = 5240$ K. The triangles and dotted lines are those for $T_{\rm eff} = 5020$ K.

Table 4. Equivalent widths of neutral iron lines used in surface gravity determination (mÅ).

Star	6082.7	6096.7	6151.6	6230.7	6232.6	6252.6	6430.8
HBC 388	77± 1	60±2	79±3	252± 5	147± 6	172± 3	188± 5
V773 Tauri	—	—	—	365±11	247±13	—	223± 8
UX Tauri	101± 2	—	96±7	285± 7	195±13	246±12	217± 5
GI Tauri	140±15	36±5	—	162± 0	122± 4	94± 4	122±13
T Tauri	111± 3	103±5	112±6	279± 8	211±11	192± 8	205± 7
DR Tauri	46± 4	39±3	—	—	—	—	—

Table 5. Equivalent widths of ionized iron lines used in surface gravity determination (mÅ).

Star	6084.1	6149.3	6238.4	6247.6	6432.7
HBC 388	20±1	50±6	54±4	62±4	63±6
V773 Tauri	—	—	60±6	—	30±5
UX Tauri	20±3	39±3	47±2	56±9	63±6
GI Tauri	23±4	—	40±4	15±5	41±6
T Tauri	20±2	41±5	36±6	32±4	24±4
DR Tauri	14±3	—	—	—	—

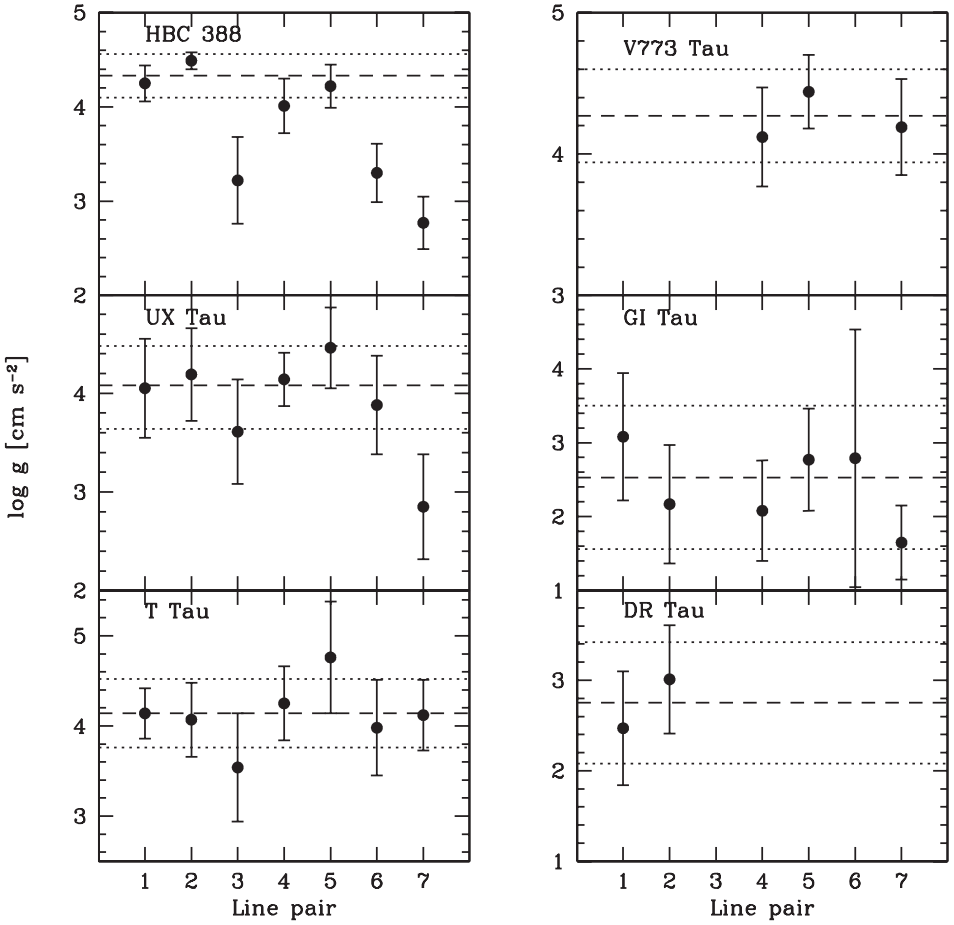

Fig. 4. Derived line-ratio surface gravities. The "Line pair" numbers correspond to the numbers in parenthesis of each fit of figure 3.

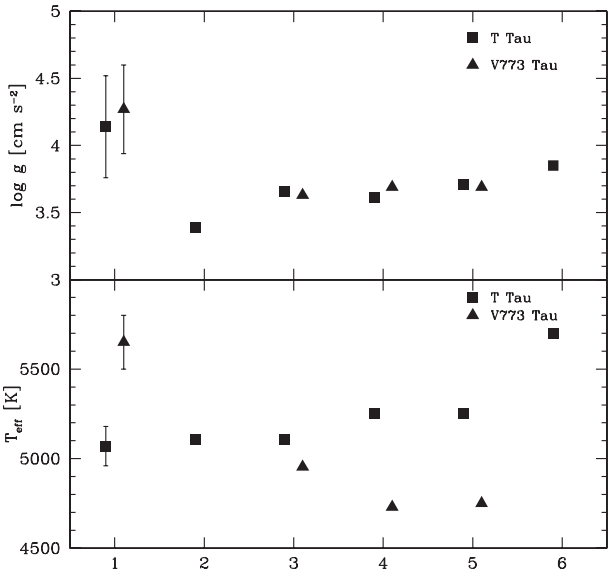

Fig. 5. Derived effective temperatures (bottom) and surface gravities (top) for T Tau and V773 Tau, along with results from the literature. 1: This work, 2: Cohen and Kuhi (1979); 3: Strom et al. (1989); 4: Kenyon and Hartmann (1995); 5: Basri et al. (1991); 6: Calvet et al. (2004).

As for the case of T Tau, the derived effective temperature is in good agreement with past results, but the surface gravity is noticeably different. The rotational velocity is mild enough, and the S/N is satisfactory, which leaves us no other factor to reason with. The "filling in" of selective absorption lines mentioned by Finkenzeller and Basri (1987) may be one of the causes. Further investigation is needed to uncover the reason for this discrepancy.

The surface gravities for DR Tau and GI Tau are unreasonably low. From the literature (Hartigan et al. 1990), we know that DR Tau is heavily veiled ($r = 8.8$), consequently making the EW measurements difficult. As for GI Tau, it is the faintest object in the sample, and the observed spectrum have a very poor S/N. Therefore, the derived surface gravities for DR Tau and GI Tau may not be of much certainty.

We thank the staff of the Okayama Astrophysical Observatory for their assistance in the observations. Yuske Taguchi is supported by the Kobe University 21st Century COE Program and the Iue Memorial Foundation Scholarship.

References

Basri, G., & Batalha, C. 1990, ApJ, 363, 654
Basri, G., Martin, E. L., & Bertout, C. 1991, A&A, 252, 625
Bell, R. A., & Gustafsson, B. 1989, MNRAS, 236, 653
Bertout, C. 1989, ARA&A, 27, 351
Bertout, C., Basri, G., & Bouvier, J. 1988, ApJ, 330, 350
Calvet, N., Muzerolle, J., Briceño, C., Hernández, J., Hartmann, L., Saucedo, J. L., & Gordon, K. D. 2004, AJ, 128, 1294
Cohen, M., & Kuhi, L. V. 1979, ApJS, 41, 743
Finkenzeller, U., & Basri, G. 1987, ApJ, 318, 823
Hartigan, P., Hartmann, L., Kenyon, S. J., Strom, S. E., & Skrutskie, M. F. 1990, ApJ, 354, L25
Hartigan, P., Kenyon, S. J., Hartmann, L., Strom, S. E., Edwards, S., Welty, A. D., & Stauffer, J. 1991, ApJ, 382, 617
Kenyon, S. J., & Hartmann, L. 1987, ApJ, 323, 714
Kenyon, S. J., & Hartmann, L. 1995, ApJS, 101, 117
Kurucz, R. L. 1993, Kurucz CD-ROM, No.13 (Cambridge: Smithsonian Astrophysical Observatory)
Padgett, D. L. 1996, ApJ, 471, 847
Schiavon, R. P., Batalha, C., & Barbuy, B. 1995, A&A, 301, 840
Siess, L., Forestini, M., & Dougados, C. 1997, A&A, 324, 556
Strom, K. M., Strom, S. E., Edwards, S., Cabrit, S., & Skrutskie, M. F. 1989, AJ, 97, 1451
Takeda, Y., Ohkubo, M., & Sadakane, K. 2002, PASJ, 54, 451